

A Novel Multi Source Electrical Energy System

Bindu.K.V¹, S.Munikrishnan²,B. Justus Rabi³

1&2.Research Scholar, 3. Research Supervisor, Anna University of Technology, Chennai, India

¹bindukv1@rediffmail.com, ²munikrishnan.2011@rediffmail.com, ³bennisrobi@rediffmail.com

Abstract:- The paper presents the new scheme of green energy systems using solar- and wind-energy systems in order to reduce the pollution in the grid. The opportunity of a large wind and solar power production is being explored and also discusses different power electronics circuits and control methods to link the renewable energy to the national grid. This paper recommends some of the modern power electronic converters applicable to hybrid power energy systems which have improved significantly in solar and wind energy technologies to improve the quality of power. A new system configuration of the front-end rectifier stage for a hybrid wind/photovoltaic energy system allows the two sources to supply the load separately or simultaneously depending on the availability of the energy sources. The inherent nature of this Cuk-SEPIC fused converter, additional input filters are not necessary to filter out high frequency harmonics. Harmonic content is detrimental for the generator lifespan, heating issues, and efficiency. The fused multi input rectifier stage also allows Maximum Power Point Tracking (MPPT) to be used to extract maximum power from the wind and sun whenever it is available. An adaptive MPPT algorithm is used for the wind system and a standard perturb and observe method is used for the PV system. Operational analysis and the simulation results are given to highlight the merits of the proposed circuit.

Keywords: Solar power, Wind energy system. Maximum Power Point Tracking.

I.INTRODUCTION

Environmental friendly solutions are becoming more prominent than ever as a result of concern regarding the state of our deteriorating planet. With increasing concern of global warming and the depletion of fossil fuel reserve looks an alternate sustainable energy solutions to preserve the earth for the future generations. Other than hydro power, wind and photovoltaic energy holds the most potential to meet our energy demands. The wind energy is capable of supplying large amounts of power but its presence is highly unpredictable [1]. Similarly, solar energy is present throughout the day but the solar irradiation levels vary due to sun intensity and unpredictable shadows cast by clouds, monsoons etc. However, by combining these two intermittent sources and by incorporating maximum power point tracking (MPPT) algorithms, the system's power transfer efficiency and reliability can be improved significantly. When a source is unavailable or insufficient in meeting the load demands, the compensation is achieved by

the other energy source. Several hybrid wind/PV power systems with MPPT control have been proposed in the literature [2]-[3] uses a separate DC/DC boost converter connected in parallel in the rectifier stage to perform the MPPT control for each the renewable energy power sources. A simpler multi input structure has been discussed by the combination of the sources from the DC-end while still achieving MPPT for each renewable source. The structure proposed is a fusion of the buck and buck-boost converter. The systems in literature [4] require passive input filters to remove the high frequency current harmonics injected into wind turbine generators [5]-[6]. In this paper, an alternative multi-input rectifier structure is proposed for hybrid wind/solar energy systems. The proposed design is a fusion of the Cuk and SEPIC converters which is shown in fig: 1. The features of the proposed topology are: 1) the inherent nature of these two converters eliminates the need for separate input filters for PFC; 2) it can support step up/down operations for each renewable source (can support wide ranges of PV and wind input); 3) MPPT can be realized for each source; 4) individual and simultaneous operation is supported

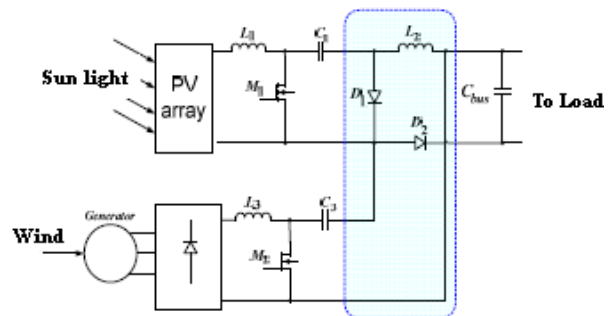


Fig 1: Fusion of the Cuk and SEPIC converters

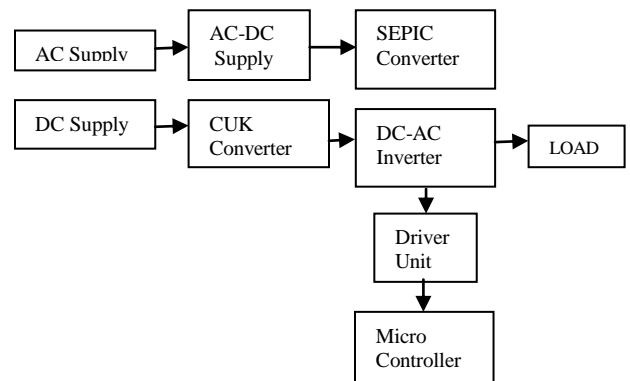


Fig: 2 Block diagram of the proposed topology

A solar cell is used to directly convert solar energy into electrical energy phenomenon of PV effect [7]. The solar modules are formed by solar stacks and the energy absorbed from the sun is converted into electrical energy which is called solar power. Fig 2 shows the block diagram of proposed topology. Cells are described as photovoltaic cells when the light source is not necessarily sunlight. Developed for over a millennium, today's wind turbines are manufactured in a range of vertical and horizontal axis types. The smallest turbines are used for applications such as battery charging or auxiliary power on sailing boats; while large grid-connected arrays of turbines are becoming an increasingly large source of commercial electric power [10]. The Cuk converter shown in Fig. 3 is a type of DC-DC converter that maintains an output voltage which is less or greater than the input voltage. The non-isolated Cuk converter can only have opposite polarity between input and output, which uses a capacitor as its main energy-storage component, unlike most other types of converters which use an inductor [11]-[12].

II. CUK CONVERTER

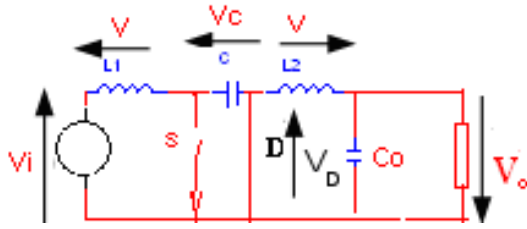


Fig 3: Schematic of a non-isolated Cuk converter

In this figure 4, the diode and the switch are either replaced by a short circuit when they are on or by an open circuit when they are off [13]. It can be seen that when in the Off state, the capacitor C is being charged by the input source through the inductor L_1 . When in the On state, the capacitor C transfers the energy to the output capacitor through the inductance L_2 . A non-isolated Cuk converter comprises two inductors, two capacitors, a switch (usually a transistor), and a diode. Its schematic can be seen in figure 4. It is an inverting converter,

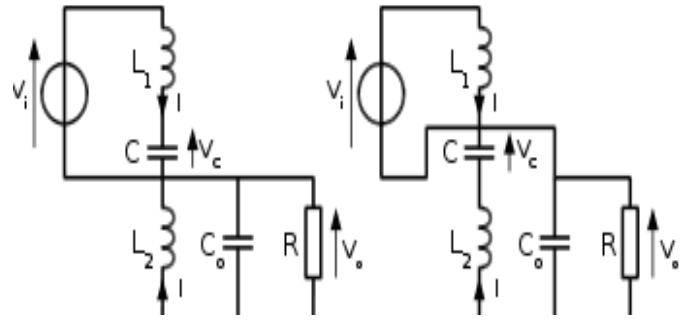


Fig 4: The two operating states of a non-isolated Cuk converter

so the output voltage is negative with respect to the input voltage. The capacitor C is used to transfer energy and is connected alternately to the input and to the output of the converter via the commutation of the transistor and the diode. The two inductors L_1 and L_2 are used to convert respectively the input voltage source (V_i) and the output voltage source (C_o) into current sources. Indeed, at a short time scale an inductor can be considered as a current source as it maintains a constant current [14]-[15]. This conversion is necessary because if the capacitor were connected directly to the voltage source, the current would be limited only by (parasitic) resistance, resulting in high energy loss. Charging a capacitor with a current source (the inductor) prevents resistive current limiting and its associated energy loss. As with other converters (buck converter, boost converter, buck-boost converter) the Cuk converter can either operate in continuous or discontinuous current mode. However, unlike these converters, it can also operate in discontinuous voltage mode (i.e., the voltage across the capacitor drops to zero during the commutation cycle).

Continuous mode: In steady state, the energy stored in the inductors has to remain the same at the beginning and at the end of a commutation cycle. The energy in an inductor is given by:

$$E = \frac{1}{2} LI^2 \quad (1)$$

This implies that the current through the inductors has to be the same at the beginning and the end of the commutation cycle. As the evolution of the current through an inductor is related to the voltage across it:

$$V_L = L \frac{dI}{dt} \quad (2)$$

It can be seen that the average value of the inductor voltages over a commutation period have to be zero to satisfy the steady-state requirements. If we consider that the capacitor C and C_o are large enough for the voltage ripple across them to be negligible, the inductor voltages become: In the off-state, inductor L_1 is connected in series with V_i . Therefore $V_{L1} = V_i - V_C$. As the diode D is forward biased (we consider zero voltage drop), L_2 is directly connected to the output capacitor. Therefore $V_{L2} = V_o$. In the on-state, inductor L_1 is directly connected to the input source. Therefore

$V_{L1} = V_i$. Inductor L_2 is connected in series with C and the output capacitor, so $V_{L2} = V_o + V_c$. The converter operates in on-state from $t=0$ to $t = D \cdot T$ and in off state from $D \cdot T$ to T (that is, during a period equal to $(1-D) T$). The average values of V_{L1} and V_{L2} are therefore:

$$V_{L1} = D \cdot V_i + (1-D) \cdot (V_i - V_c) = (V_i - (1-D) \cdot V_c) \quad (3)$$

As both average voltage have to be zero to satisfy the steady-state conditions we can write, using the last equation:

$$V_c = - (V_o/D) \quad (4)$$

So the average voltage across L_1 becomes:

$$V_{L1} = \{V_i + (1-D) \cdot V_o/D\} = 0 \quad (5)$$

$$V_{L2} = D (V_o + V_c) + (1-D) \cdot V_o = (V_o + D \cdot V_c) \quad (6)$$

Which can be written as:

$$V_o/V_i = - [D/ (1-D)] \quad (7)$$

It can be seen that this relation is the same as that obtained for the Buck-boost converter.

Discontinuous mode

$$P_i = P_o \quad (8)$$

Inductor coupling: Instead of using two discrete inductor components, many designers implement a coupled inductor Cuk converter, using a single magnetic component that includes both inductors on the same core. The transformer action between the inductors inside that component gives a coupled inductor Cuk converter lower output ripple than a Cuk converter using two independent discrete inductor components.

III. SINGLE-ENDED PRIMARY-INDUCTOR (SEPIC) CONVERTER

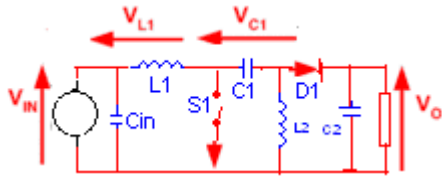


Fig 5: Single-ended primary-inductor converter

Single-ended primary-inductor converter (SEPIC) as shown in fig: 5 is a type of DC-DC converter allowing the electrical potential (voltage) at its output to be greater than, less than, or equal to that at its input; the output of the SEPIC is controlled by the duty cycle of the control transistor. A SEPIC is similar to a traditional buck-boost converter, but has advantages of having non-inverted output (the output voltage is of the same polarity as the input voltage), the isolation between its input and output (provided by a capacitor in series), and true shutdown mode: when the switch is turned off, its output drops to 0 V. SEPICs are useful in applications in which a battery voltage can be above and below that of the regulator's intended output. As with other SMPS the SEPIC exchanges energy between the capacitor and inductors in order to convert from one the capacitor and inductors in order

to convert from one the capacitor and inductors in order to convert from one switched mode power supplies the SEPIC exchanges energy between the capacitor and inductors in order to convert from one voltage to another. The amount of energy exchanged is controlled by switch $S1$, which is typically a transistor such as a MOSFET; MOSFETs offer much higher input impedance and lower voltage drop than bipolar junction transistors (BJTs), and do not require biasing resistors (as MOSFET switching is controlled by differences in voltage rather than a current, as with BJTs).

Continuous mode: A SEPIC is said to be in continuous-conduction mode ("continuous mode") if the current through the inductor $L1$ never falls to zero. Fig 6 shows with $S1$ open current through $L1$. During a SEPIC's steady-state operation, the average voltage across capacitor $C1$ (V_{C1}) is equal to the input voltage (V_{in}). Because capacitor $C1$ blocks direct current (DC), the average current across it (I_{C1}) is zero, making inductor $L2$ the only source of load current. Therefore, the average current through inductor $L2$ (I_{L2}) is the same as the average load current and hence independent of the input voltage. Looking at average voltages, the following can be written:

$$V_{IN} = V_{L1} + V_{C1} + V_{L2} \quad (9)$$

Because the average voltage of V_{C1} is equal to V_{IN} , $V_{L1} = -V_{L2}$. For this reason, the two inductors can be wound on the same core. Since the voltages are the same in magnitude, their effects of the mutual inductance will be zero, assuming the polarity of the windings is correct. Also, since the voltages are the same in magnitude, the ripple currents from the two inductors will be equal in magnitude. The average currents can be summed as follows:

$$I_{D1} = I_{L1} - I_{L2} \quad (10)$$

When switch $S1$ is turned on, current I_{L1} increases and the current I_{L2} increases in the negative direction. The energy to increase the current I_{L1} comes from the input source, since $S1$ is a short while closed, and the instantaneous voltage V_{C1} is approximately V_{IN} , the voltage V_{L2} is approximately $-V_{IN}$. Therefore, the capacitor $C1$ supplies the energy to increase the magnitude of the current in $L2$ and thus increase the energy stored in $L2$. The easiest way to visualize this is to consider the bias voltages of the circuit in a dc state, and then close $S1$. When switch $S1$ is turned off, the current I_{C1} becomes the same as the current I_{L1} , since inductors do not allow instantaneous changes in current. The current I_{L2} will continue in the negative direction, in fact it never reverses direction. It can be seen from the diagram that a negative I_{L2} will add to the current I_{L1} to increase the current delivered to the load. Using Kirchoff's Current Law, it can be shown that $I_{D1} = I_{C1} - I_{L2}$. It can then be concluded, that while $S1$ is off, power is delivered to the load from both $L2$ and $L1$. $C1$, however is being charged by $L1$ during this off cycle, and will in turn recharge $L2$ during the on cycle. Because the potential (voltage) across capacitor $C1$ may

reverse direction every cycle, a capacitor should be used.

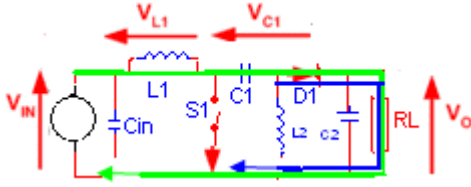


Fig 6: With S1 open current through L1 (green) and current through L2 (red) produce current through the load

The voltage across capacitor C1 will not change unless the switch is closed long enough for a half cycle of resonance with inductor L2, and by this time the current in inductor L1 could be quite large. The capacitor C_{IN} is required to reduce the effects of the parasitic inductance and internal resistance of the power supply. The boost/buck capabilities of the SEPIC are possible because of capacitor C1 and inductor L2. Inductor L1 and switch S1 create a standard boost converter, which generate a voltage (V_{S1}) that is higher than V_{IN}, whose magnitude is determined by the duty cycle of the switch S1. Since the average voltage across C1 is V_{IN}, the output voltage (V_O) is V_{S1} - V_{IN}. If V_{S1} is less than 2V_{IN}, then the output voltage will be less than the input voltage. If V_{S1} is greater than 2V_{IN}, then the output voltage will be greater than the input voltage. The evolution of switched-power supplies can be seen by coupling the two inductors in a SEPIC converter together, which begins to resemble a fly-back converter, the most basic of the transformer-isolated SMPS topologies.

The voltage drop and switching time of diode D1 is critical to a SEPIC's reliability and efficiency and the converter will operate in discontinuous mode. The diode's switching time needs to be extremely fast in order to avoid high voltage spikes across the inductors, which could cause damage to components. The resistances in the inductors and the capacitor can also have large effects on the converter efficiency and ripple. Inductors with lower series resistance allow less energy to be dissipated as heat, resulting in greater efficiency.

IV. PROPOSED MULTI-INPUT RECTIFIER STAGE MULTI-INPUT RECTIFIER STAGE

The fusion of the two converters is achieved by reconfiguring the two existing diodes from each converter and the shared utilization of the Cuk output inductor by the SEPIC converter. This configuration allows each converter to operate individually when one source is available. Figure 7 illustrates the case when only the wind source is available and in this case, D1 turns off and D2 turns on; the proposed circuit becomes a SEPIC converter and the input to output voltage relationship is given by equation (1). On the other hand, if only the solar source is available, then D2 turns off and D1 will always be on and the circuit becomes a Cuk converter as shown in Figure 8. The input to output voltage relationship is given by equation (2). In both cases, the converters have step-up/down capability, which provide more

design flexibility in the system if duty ratio control is utilized to perform MPPT control.

$$V_{dc}/V_w = d_2 / (1-d_2) \quad (11)$$

$$V_{dc}/V_{pv} = d_1 / (1-d_1) \quad (12)$$

Modes of operation: State I, II, IV. Similarly, the switching states will be state I, III, IV if the switch conduction periods are vice versa. To provide a better explanation, the inductor current waveforms of each switching state are given as follows assuming that $d_2 > d_1$; hence only states I, III, IV are discussed in fig 8. In the following, $I_{i,pv}$ is the average input current from the PV source; $I_{i,w}$ is the RMS input current after the rectifier (wind case); and I_{dc} is the average system output current. The key waveforms that illustrate the switching states are shown in Figure 10. The mathematical expression that relates the total output voltage and the two input sources are illustrated.

State I (M1 on, M2 on):

$$I_{L1} = I_{i,pv} + [(V_{pv}/L_1)t] \quad 0 < t < d_1 T_s \quad (13)$$

$$I_{L2} = I_{dc} + [(v_{c1} + v_{c2})/L_2] t \quad 0 < t < d_1 T_s \quad (14)$$

$$I_{L3} = I_{i,w} + [(V_w)/L_2] t \quad 0 < t < d_1 T_s \quad (15)$$

State III (M1 off, M2 on):

$$I_{L1} = I_{i,pv} + [(V_{pv} + v_{c1})/L_1] t \quad d_1 T_s < t < T_s \quad (16)$$

$$I_{L2} = I_{dc} + [(V_{c2})/L_2] t \quad d_1 T_s < t < T_s \quad (17)$$

$$I_{L3} = I_{i,w} + [(V_w)/L_3] t \quad d_1 T_s < t < T_s \quad (18)$$

State IV (M1 off, M2 off):

$$I_{L1} = I_{i,pv} + [(V_{pv} - v_{c1})/L_1] t \quad d_2 T_s < t < T_s \quad (19)$$

$$I_{L2} = I_{dc} - [(V_{dc})/L_2] t \quad d_2 T_s < t < T_s \quad (20)$$

$$I_{L3} = I_{i,w} + [(V_w - v_{c2} - V_{dc})/L_3] t \quad d_1 T_s < t < d_2 T_s \quad (21)$$

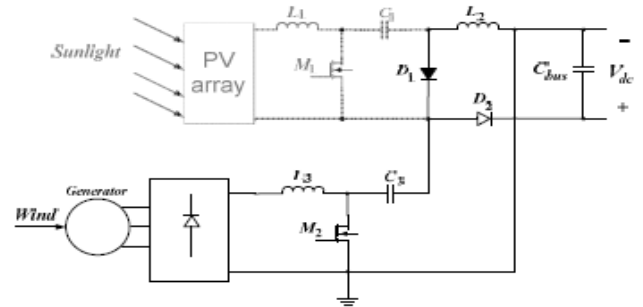


Fig 7: only wind source is operational (SEPIC)

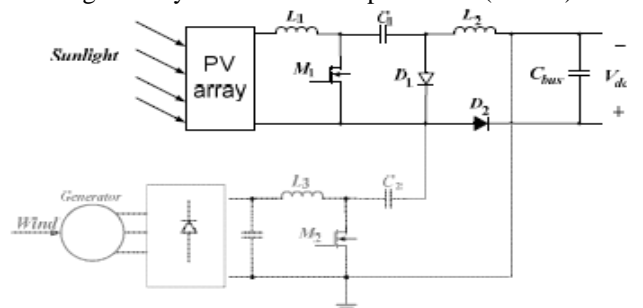
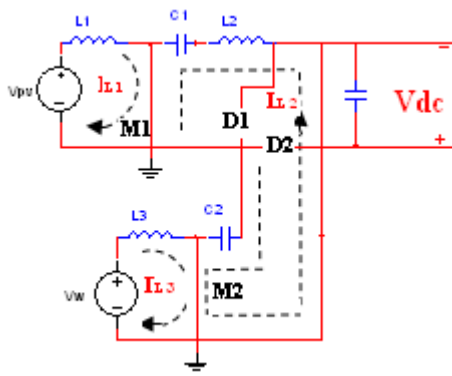
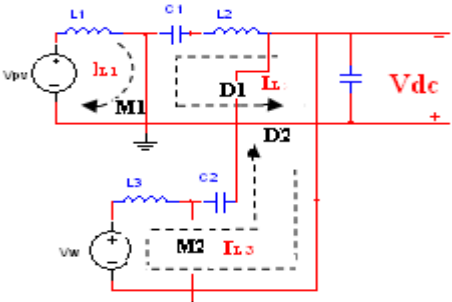


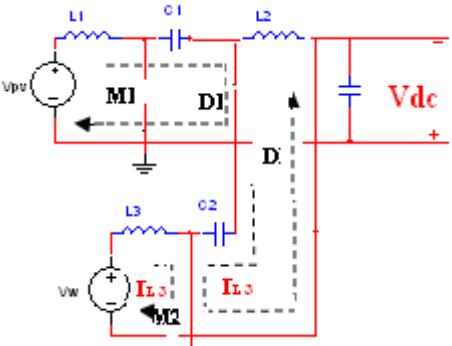
Fig 8: Only PV source is operation (Cuk)



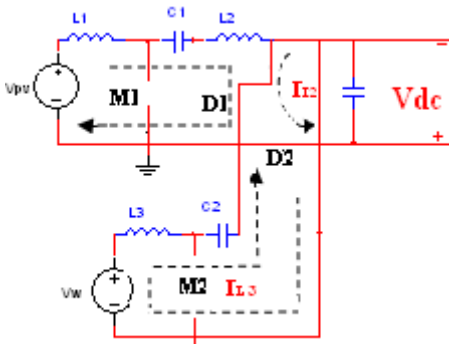
State I (M1 on, M2 on)



M1 On, M2 off



M1 OFF, M2 ON



M1 off, M2 off

Fig 9: Modes of operation

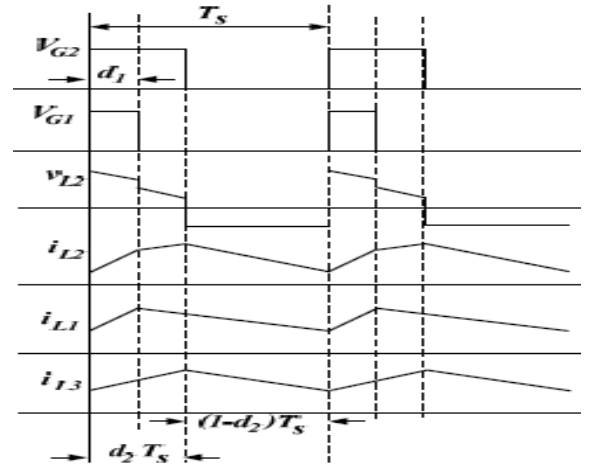


Fig 10: switching states within a switching cycle

V. VOLTAGE O/P OF CUK & SEPIC CONVERTERS

The expression for the output DC bus voltage, V_{dc} , the volt-balance of the output inductor, L_2 , is examined with $d_2 > d_1$. Since the net change in the voltage of L_2 is zero, applying volt-balance to L_2 results in. The expression that relates the average output DC voltage (V_{dc}) to the capacitor voltages (v_{c1} and v_{c2}) is then obtained as shown in , where v_{c1} and v_{c2} can then be obtained by applying volt-balance to L_1 and L_3 . The final expression that relates the average output voltage and the two input sources (V_W and V_{PV}) is then given by (5). It is observed that V_{dc} is simply the sum of the two output voltages of the Cuk and SEPIC converter. This further implies that V_{dc} can be controlled by d_1 and d_2 individually or simultaneously.

$$(v_{c1} + v_{c2}) d_1 T_1 + (v_{c2}) (d_2 - d_1) T_2 + (1-d_2) (-V_{dc}) T_2 = 0 \quad (22)$$

$$V_{dc} = [d_1 / (1-d_2)] v_{c1} + [d_2 (1-d_2)] v_{c2} \quad (23)$$

$$V_{dc} = [d_1 / (1-d_1)] V_{pv} + [d_2 (1-d_2)] V_{pv} \quad (24)$$

The switches voltage and current characteristics are also provided in this section. The voltage stress is given by (6) and (7) respectively. As for the current stress, it is observed from Figure 6 that the peak current always occurs at the end of the on-time of the MOSFET. Both the Cuk and SEPIC MOSFET current consists of both the input current and the capacitor (C_1 or C_2) current. The peak current stress of M_1 and M_2 are given by (8) and (10) respectively. L_{eq1} and L_{eq2} , given by (9) and (11), represent the equivalent inductance of Cuk and SEPIC converter respectively. The PV output current, which is also equal to the average input current of the Cuk converter, is given in (12). It can be observed that the average inductor current is a function of its respective duty cycle (d_1). Therefore by adjusting the respective duty cycles for each energy source, maximum power point tracking can be achieved.

VI. MPPT CONTROL OF PROPOSED CIRCUIT

A common inherent drawback of wind and PV systems is the intermittent nature of their energy sources. Wind energy is capable of supplying large amounts of power but its presence

is highly unpredictable as it can be here one moment and gone in another. Solar energy is present throughout the day, but the solar irradiation levels vary due to sun intensity and unpredictable shadows cast by clouds, birds, trees, etc. These drawbacks tend to make these renewable systems inefficient. However, by incorporating maximum power point tracking (MPPT) algorithms, the systems' power transfer efficiency can be improved significantly. To describe a wind turbine's power characteristic, equation describes the mechanical power that is generated by the wind. The Mechanical Power Produced by Wind is given by

$$P_m = 0.5\rho AC_p(\lambda,\beta)v_w^3 \quad (25)$$

Where

ρ = air density,

A = rotor swept area,

$C_p(\lambda,\beta)$ = power coefficient function,

λ = tip speed ratio,

β = pitch angle,

v_w = wind speed

The power coefficient (C_p) is a nonlinear function that represents the efficiency of the wind turbine to convert wind energy into mechanical energy. It is dependent on two variables, the tip speed ratio (TSR) and the pitch angle. The TSR, λ , refers to a ratio of the turbine angular speed over the wind speed. The mathematical representation of the TSR [10] is given by equation (14). The pitch angle, β , refers to the angle in which the turbine blades are aligned with respect to its longitudinal axis.

$$\lambda = R \omega_b / v_w \quad (26)$$

where R= turbine radius,

ω_b = angular rotational speed

Figure 11 and 12 are illustrations of a power coefficient curve and power curve for a typical fixed pitch ($\beta = 0$) horizontal axis wind turbine. From the power curves for each wind speed has a shape similar to that of the power coefficient curve. Because the TSR is a ratio between the turbine rotational speed and the wind speed, it follows that each wind speed would have a different corresponding optimal rotational speed that gives the optimal TSR. For each turbine there is an optimal TSR value that corresponds to a maximum value of the power coefficient ($C_{p,max}$) with maximum power. Therefore by controlling rotational speed, maximum power can be obtained for different wind speeds.

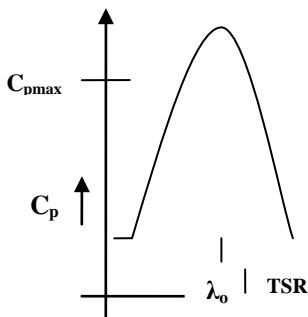


Fig 11: Power Coefficient Curve for a typical wind turbine

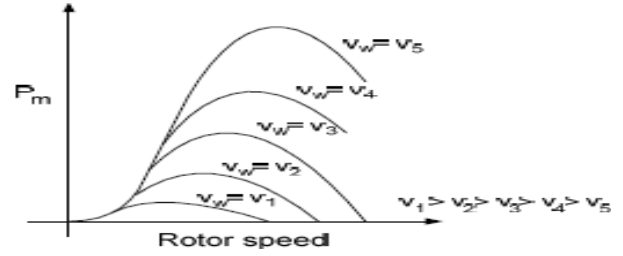


Fig 12: Power Curves for a typical wind turbine.

PV arrays produce currents via the photovoltaic effect. PV arrays are constructed by placing numerous solar cells connected in series and in parallel [5]. The current-voltage characteristic of a solar cell is derived as follows:

$$I = I_{ph} - I_D$$

$$I = I_{ph} - I_0 \{ \exp [q (V + R_s I) / A k_B T] - 1 \} - (V + R_s I) / R_{sh}$$

Where I_{ph} = photocurrent,

I_D = diode current,

I_0 = saturation current,

A = ideality factor,

q = electronic charge 1.6×10^{-19} ,

k_B = Boltzmann's gas constant (1.38×10^{-23}),

T = cell temperature,

R_s = series resistance,

R_{sh} = shunt resistance,

I = cell current,

V = cell voltage

VII. PROPOSED MODULATION TECHNIQUE

Due to the similarities of the shape of the wind and PV array power curves, a similar maximum power point tracking scheme known as the hill climb search strategy is often applied to these energy sources to extract maximum power. The HCS strategy perturbs the operating point of the system observes the output. If the direction of the perturbation results in a positive change in the output power, then the control algorithm will continue in the direction of the previous perturbation. Conversely, if a negative change in the output power is observed, then the control algorithm will reverse the direction of the previous perturbation step. In the case that the change in power is close to zero (within a specified range) then the algorithm will invoke no changes to the system operating point since it corresponds to the maximum power point (the peak of the power curves)

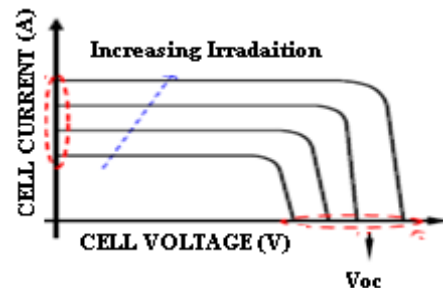


Fig 13: typical output power characteristics of a PV array

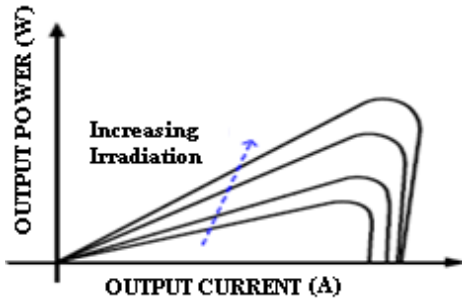


Figure 14: PV cell power characteristics

The MPPT scheme implemented in this paper is explained by the flow chart shown in Figure 15. In the proposed inverter circuit the multi carrier modulation technique is employed, which will invoke no changes to the system operating point since it corresponds to the maximum power point. These are the classical and most widely used methods of pulse width modulation. They have as common characteristic sub cycles of constant time duration, a sub cycle being defined as the total duration T_s during which an active inverter leg assumes two consecutive switching states of opposite voltage polarity.

Operation at sub cycles of constant duration is reflected in the harmonic spectrum by two salient sidebands, centered around the carrier frequency, and additional frequency bands around integral multiples of the carrier. The multi carrier modulation technique is very suitable for a multilevel inverter circuit. By employing this technique along with the multilevel topology, the low THD output waveform without any filter circuit is possible. Switching devices, in addition, turn on and off only one time per cycle which can overcome the switching loss problem, as well as EMI problem. These are the classical and most widely used methods of pulse width modulation. They have common characteristic sub cycles of constant time duration, a sub cycle being defined as the total duration T_s during which an active inverter leg assumes two consecutive switching states of opposite voltage polarity. Operation at sub cycles of constant duration is reflected in the harmonic spectrum by two salient sidebands, centered around the carrier frequency, and additional frequency bands around integral multiples of the carrier. for a multilevel inverter circuit. By this technique along with the multilevel topology, the low THD output waveform without any filter circuit is possible. Switching devices, in addition, turn on and off only one time per cycle which can overcome the switching loss problem, as well as EMI problem.

VIII. SIMULATION RESULTS

In this section, simulation results from PSIM 8.0.7 is given to verify that proposed multi-input rectifier stage can support individual as well as simultaneous operation. The specifications for the design example are given in TABLE I. Figure 14 illustrates the system under the condition where the wind source has failed and only the PV source (Cuk converter mode) is supplying power to the load. Figure 15 illustrates the system where only the wind turbine generates power to the

load (SEPIC converter mode). Finally, Figure 16 illustrates the simultaneous operation (Cuk-SEPIC fusion mode) of the two sources where M2 has a longer conduction cycle

TABLE I. Design Specifications

Output Power(W)	3 Kw
Output Voltage	500 V
Switching Frequency	20kHz

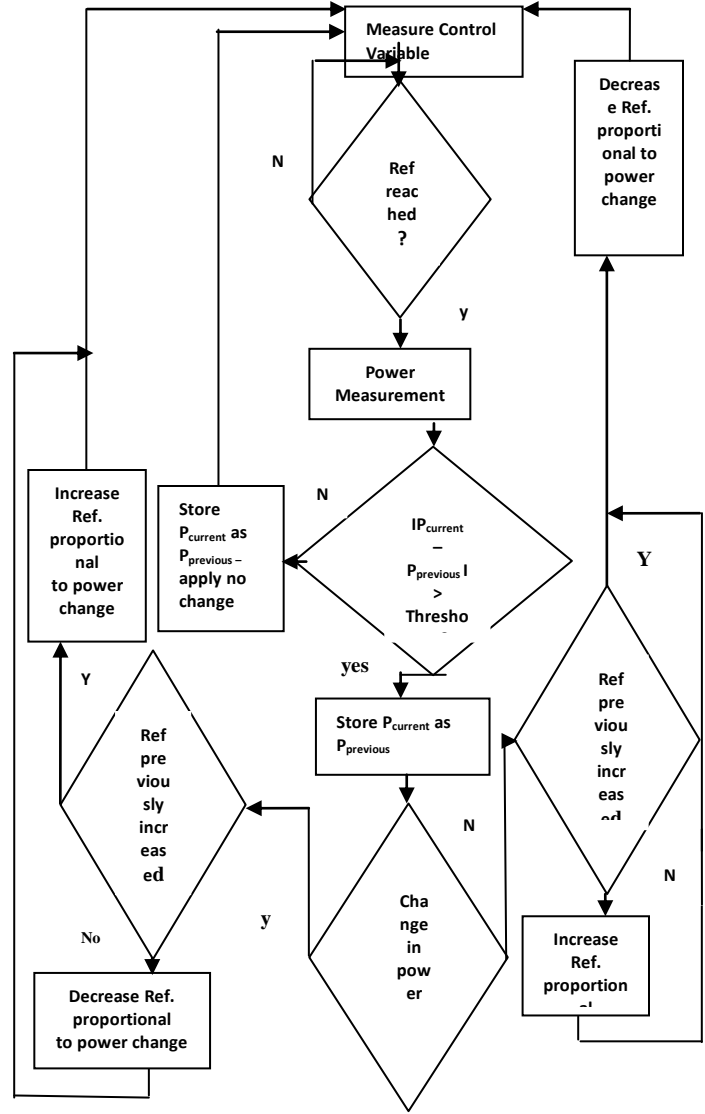


Fig 15: General MPPT Flow Chart for wind and PV

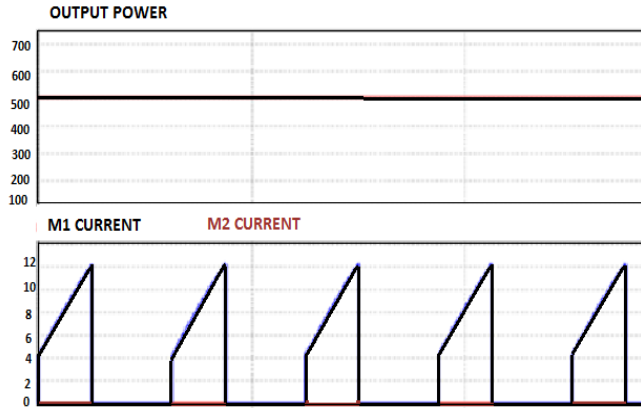


Fig 16: Individual operation with only PV source (Cuk operation) Top: Output power, Bottom: Switch currents (M1 and M2)

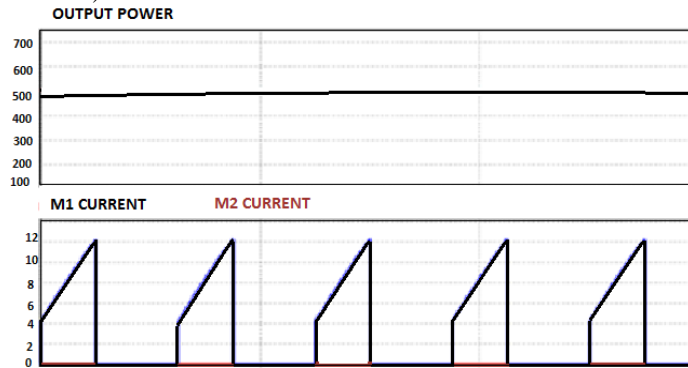


Fig 17: Individual operation with only wind source (SEPIC operation) (I) The injected three phase generator current; (II) Top: Output power, Bottom: Switch currents (M1 and M2)

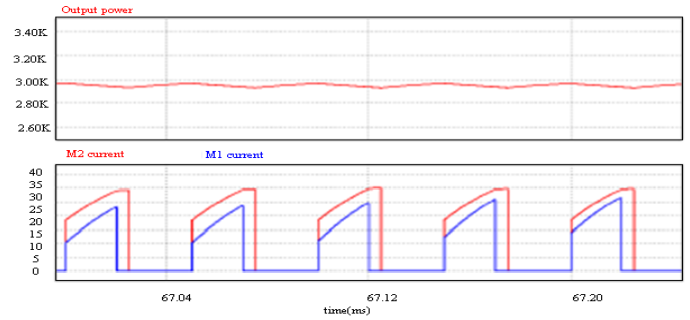
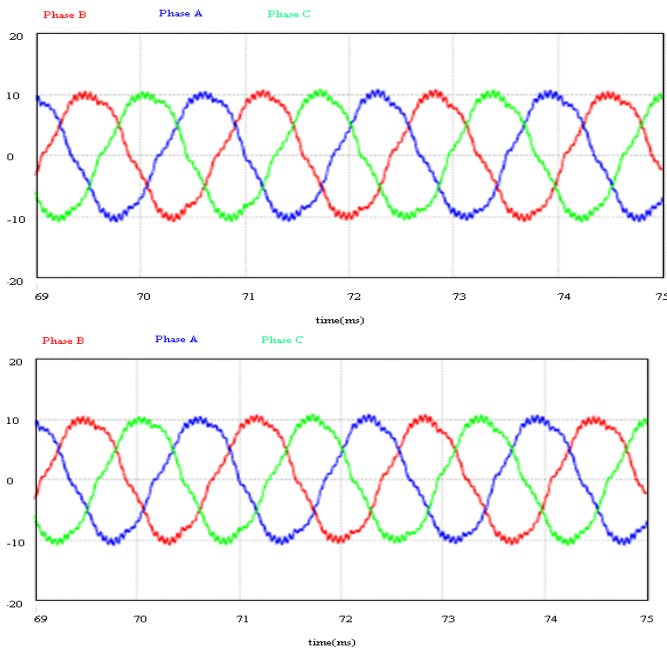


Fig 18: Simultaneous operation with both wind and PV source (Fusion mode with Cuk and SEPIC) (I) The injected three phase generator current; (II) Top: Output power, Bottom: Switch currents (M1 and M2)

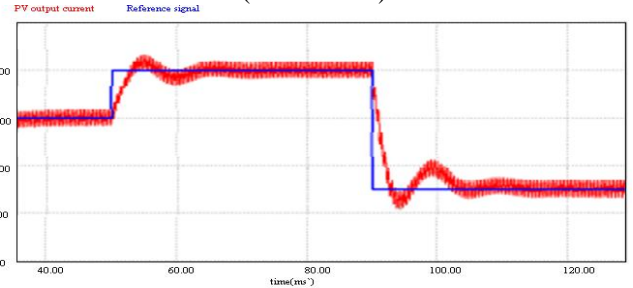


Fig 19: Solar MPPT – PV output current and reference current signal (Cuk operation)

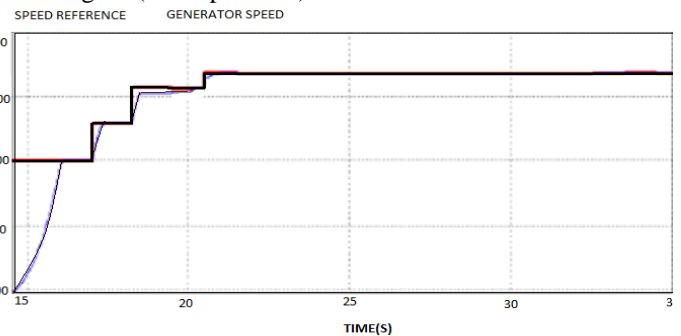


Fig 20: Wind MPPT – Generator speed and reference speed signal (SEPIC operation)

IX. CONCLUSION

A novel hybrid rectifier composed by the parallel combination of Cuk-SEPIC converters in fusion mode was simulated, designed and verified on proposed considerations. In the proposed system when one source is supplying power to the load, the simultaneous operation of Cuk-SEPIC fusion mode of the two sources is achieved. The inherent nature of this Cuk-SEPIC fused converter is that additional input filters are not necessary to filter out high frequency harmonics. The simulation results are given to verify that proposed multi-input rectifier stage can support individual as well as simultaneous operation. The adopted control strategy allows the regulation of the output voltage and the control of the input currents. The features of the proposed topology are the inherent nature of these two converters eliminates the need for separate input filters for PFC, it can support step up/down operations for each renewable source ,can support wide

ranges of PV and wind input, MPPT can be realized for each source, individual and simultaneous operation is supported.

REFERENCES

- [1] M. D. Manjrekar, P. K. Steimer, and T. A. Lipo, "Hybrid multilevel power conversion system: A competitive solution for high-power application," *IEEE Trans. Ind. Applicat.*, vol. 36, pp. 1565–1572, May/June 2000.
- [2] M. Song, T.-J. Tarn, and N. Xi, "Integration of task scheduling, action planning, and control in robotic manufacturing," *Proc. IEEE*, vol. 88, pp. 1097–1107, July 2000.
- [3] J. Wang, "Fundamentals of erbium-doped fiber amplifiers arrays (Periodical style—Submitted for publication)," *IEEE J. Quantum Electron.*, submitted for publication.
- [4] Smets, F. and R. Wouters (2003): "An Estimated Stochastic General Equilibrium Model of the Euro Area," *Journal of the European Economic Association*, vol. 1(5), 1123-1175.
- [5] Smets, F. and R. Wouters (2004) "Shocks and Frictions in US Business Cycles: a Bayesian DSGE Approach," mimeo.
- [6] Surendra Kumar S and Partha Sarathi Sensarma, "A multiband shunt hybrid active filter with sensorless control", *Journal of Power Electronics*, Vol. 8, No. 4, October 2008, pp. 317-324 (ISSN 1598-2092)
- [7] Samir Hazra and Partha Sarathi Sensarma, "DC Bus voltage build up and control in stand-alone wind energy conversion system using direct vector control of SCIM", *Proc. of IEEE-IECON'08, Orlando, USA, Nov. 2008*
- [8] J Santosh K Tripathi, M. Nasim and R.S. Anand, "Hybrid Semiconductor Nanocrystals-Polymer Solar Cell ", *Proc. of NCETPEGU ,2008, IIT Kanpur* , 44-45
- [9] S. Chen, B. Mulgrew, and P. M. Grant, "A clustering technique for digital communications channel equalization using radial basis function networks," *IEEE Trans. Neural Networks*, vol. 4, pp. 570–578, Jul. 1993.
- [10] A. Siebert, A. Troedson, S. Ebner, "AC to DC power conversion now and in the future", *IEEE Transactions on Industry Applications*, vol. 38, no. 4, pp. 934-940, July/August 2002.
- [11] F. J. M. Seixas, I. Barbi, "A robust 12kW three-phase rectifier using a 18-pulse autotransformer and isolated DC-DC converters", in *Proc. Of 6th Brazilian Power Electronics Conference, Florianopolis-Brazil, 2001*, vol. 2, pp. 686-691.
- [12] S. P. Bingulac, "On the compatibility of adaptive controllers (Published Conference Proceedings style)," in *Proc. 4th Annu. Allerton Conf. Circuits and Systems Theory*, New York, 1994, pp. 8–16.
- [13] G. R. Faulhaber, "Design of service systems with priority reservation," in *Conf. Rec. 1995 IEEE Int. Conf. Communications*, pp. 3–8.
- [14] L. C. G. de Freitas, M. G. Simões, C. A. Canesin, L. C. de Freitas. "A novel programmable PFC based hybrid rectifier for ultra clean power application", in *Proc. of the 35th Annual IEEE Power Electronics Specialists Conference, Aachen-Germany, 2004*, pp. 2172-2177.
- [15] R. L. Alves, C. H. Illa Font and I. Barbi. "Novel Unidirectional Hybrid Three-phase Rectifier System Employing Boost Topology" in *Proc. Of the 35th Annual IEEE Power Electronics Specialists Conference, Aachen-Germany, 2005*, pp. 487-493.